

# Control of Atomic Force Microscope Based on the Fuzzy Theory

Amir Farrokh Payam<sup>1</sup>, Eihab M. Abdel Rahman<sup>2</sup> and Morteza Fathipour<sup>1</sup>  
<sup>1</sup>Nanoelectronics Center of Excellence, Department of Electrical and Computer Engineering,  
University of Tehran, Tehran  
<sup>2</sup>Department of Systems Design Engineering, University of Waterloo, Waterloo, ON  
<sup>1</sup>Iran  
<sup>2</sup>Canada

## 1. Introduction

The atomic force microscope (Binnig *et al.*, 1986) utilizes a sharp tip moving over the surface of a sample in a raster scan mode to measure the topography and material properties of the surface. The tip is located at the free end of a cantilever microbeam (probe) which bends in response to the interaction forces between the tip and the sample. An estimate of the microbeam stiffness is used to determine the interaction forces from measurements of these deflections.

A precision positioning device, usually made of a piezoelectric tube, is used to move the tip or the sample. AFMs can be operated in one of two principal modes: (i) with feedback control or (ii) without feedback control. Though widely practiced, open-loop operation has the potential for chaotic probe tip response, thus rendering erroneous topographical information. Therefore, in a typical imaging operation the cantilever deflection is maintained at a set point by means of a feedback controller, while scanning the sample surface. The control effort is used as a measure of the sample surface profile. Actuator creep, hysteresis, probe vibrations, modeling errors, and nonlinearities are major sources of error in AFM measurements (Barret & Quate, 1991; Devasia *et al.*, 2007; Jung & Gwon, 2000).

In addition to analytical methodologies for compensation of the above mentioned errors, feedback control strategies have been developed in order to improve AFM region of operation. Conventional PD, PI, and PID feedback controllers of the AFM probe were presented in (Ashhab *et al.*, 1999) and (Sinha, 2005). Two nonlinear control techniques using a learning-based algorithm were presented in (Fang *et al.*, 2005).  $H_\infty$  and Glover-McFarlane controllers (Sebastian *et al.*, 2003), (Salapaka *et al.*, 2005) were also designed to achieve high bandwidth and robustness during AFM scanning. Other controllers based on inverse model control and combinations of feedforward and feedback and  $L_1$  and  $H_\infty$  controllers were proposed to increase the scanning speed and overcome nonlinear effects in piezoelectric actuation (Jalili *et al.*, 2004; Leang & Devasia, 2007; Pao *et al.*, 2007; Rafai & Toumi, 2004; Salapaka *et al.*, 2002; Schitter *et al.*, 2004; Schitter *et al.*, 2004; Sebastian *et al.*, 2007).

Although these methods can overcome modeling errors and have the robustness to overcome some parameter variations, they provide limited vibration compensation. In addition, in most of these methods, design complexity is combined with the use of linear

system models extracted from experimentally-measured frequency-response curves. For this reason, they neglect the nonlinear dynamics of the system and the control system is only locally stable.

The design of fuzzy controllers is simpler and faster than conventional controllers, especially in the presence of nonlinear dynamics or uncertainties where the system is not a well-posed linear system. Fuzzy control handles the nonlinearities and uncertainties of the system using rules, membership functions, and the inference process. In addition, when uncertainties or complex dynamics, which can not be modeled easily, are present in the system, the use of a fuzzy system to model the system and design the controller gives the designer the ability to implement the controller on a simple system model and extend it later to more complex or more practical systems. Moreover, fuzzy controller has an improved performance, a simpler implementation, and a reduced design and implementation cost.

In this chapter, we present an efficient PD-fuzzy controller that improves the operating characteristics of AFMs by increasing the bandwidth of the feedback controller, thereby allowing for faster scan rates and higher resolutions. We present the AFM system model in section 2, a basic fuzzy controller in section 3, our hybrid PD-fuzzy controller in section 4, and a comparative study for the performance of the two controllers and a high-gain PD controller proposed in (Leang & Devasia, 2007) in section 5. Finally, in section 6 we provide concluding remarks.

## 2. System model

The dynamics of the probe-sample system in an AFM can be modeled by the following lumped-mass system (Sinha, 2005):

$$m\ddot{x} + b\dot{x} + kx + F(x) = u \quad (1)$$

where  $x$  denotes the tip displacement,  $m$ ,  $b$ , and  $k$  denote the probe mass, damping coefficient, and stiffness, respectively,  $u(t)$  represents the controller force input, and  $F(x)$  denotes the interaction forces between the tip and surface defined by (Ashhab *et al.*, 1999):

$$F(x) = \frac{Dk}{(z_0 + x)^2} - \frac{\sigma^6 Dk}{30(z_0 + x)^8} \quad (2)$$

$z_0$  is the cantilever tip equilibrium position,  $\sigma$  denotes the molecular diameter,  $D$  is defined as:

$$D = \frac{A_H R}{6k} \quad (3)$$

$A_H$  is the Hamaker constant, and  $R$  is the tip radius. A schematic of the probe and sample system is shown in Figure 1.

The tip displacement  $x(t)$  is measured with respect to the equilibrium position  $z_0$ . To prevent contact between the tip and the surface, it is constrained by following inequality [5]:

$$(z_0 + x) \geq R \quad (4)$$

A block diagram of the AFM feedback control system is shown in Figure 2.

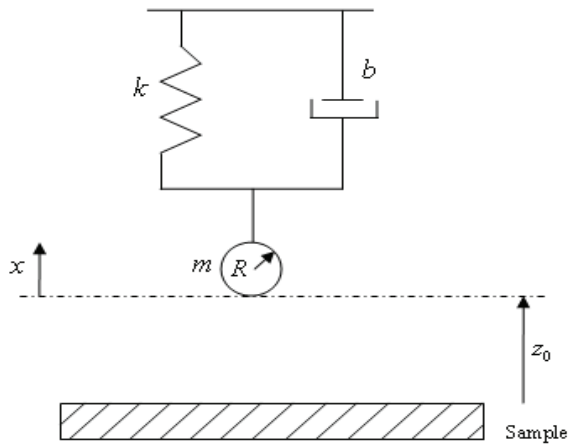


Fig. 1. A schematic of the AFM as a 1-DOF harmonic oscillator.

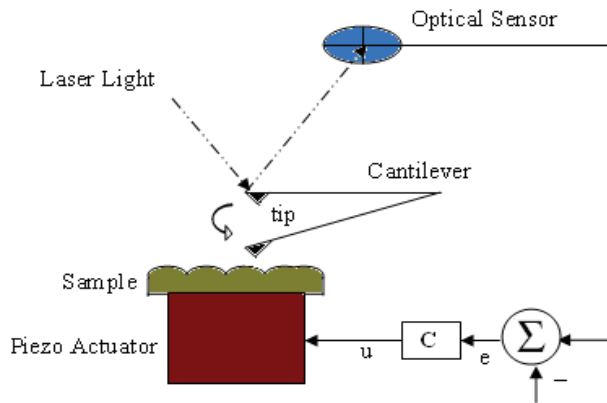


Fig. 2. A schematic of the AFM feedback control system.

### 3. Design of the basic fuzzy controller

The first step in the design of the fuzzy controller is to determine the inputs and outputs of the fuzzy system. The error between the reference and actual tip position  $e(t)$  and its time derivative  $\dot{e}(t)$  are taken as the system inputs and the controller input force  $u(t)$  is taken as the fuzzy system output. The linguistic variables listed in table 1 are chosen to represent the size of the inputs and output. The shape of membership functions of these rules has a key role in the controller design. Although trapezoidal and bell-curve functions are used in fuzzy control systems, the triangular function is computationally simpler. Other important factors in the design membership functions are the number of curves and their position. The membership functions for each linguistic variable are shown in Figures 3-5. The inputs/output is normalized to vary between -1 and 1 using the scaling boxes Gain(i) and G(i) in the Simulink diagrams, Figures 6 and 7, respectively. The membership functions for

the linguistic variables “PS” and “NS” strongly influence the steady state error of the system, whereas the membership functions for the linguistic variables “NB” and “PB” strongly influence the initial undershoot and overshoot, respectively, following a disturbance. The control surface, Figure 3, shows the operation of the fuzzy controller schematically. The magnitude of the controller input force is strongly influenced by both the error and the derivative error.

The rules commanding the fuzzy system response (output) are given in table 2. For example, when the error between the reference and actual tip position and its derivative are “small negative” and “small positive”, respectively, the output of the fuzzy controller is a “negative small” force. We selected Mamdani method to design the fuzzy inference engine using “min-function” for “and-method”, “max-function” for “or-method”, and aggregation. The “bisector-method” was used for defuzzification; that is to transform the fuzzy output to a crisp output.

NB	Negative Big
NS	Negative Small
PS	Positive Small
PB	Positive Big

Table 1. Linguistic Variables for Input/Output.

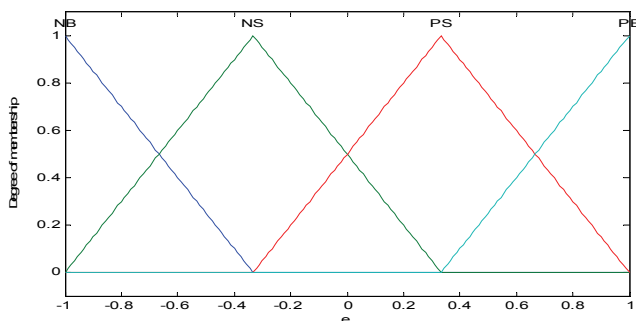


Fig. 3. Error  $e(t)$  and input force  $u(t)$  membership functions.

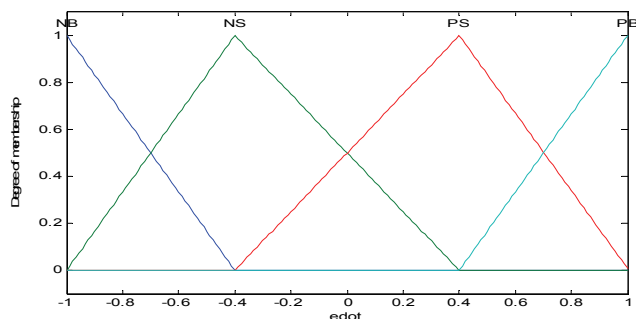


Fig. 4. Error derivative  $\dot{e}(t)$  membership function.

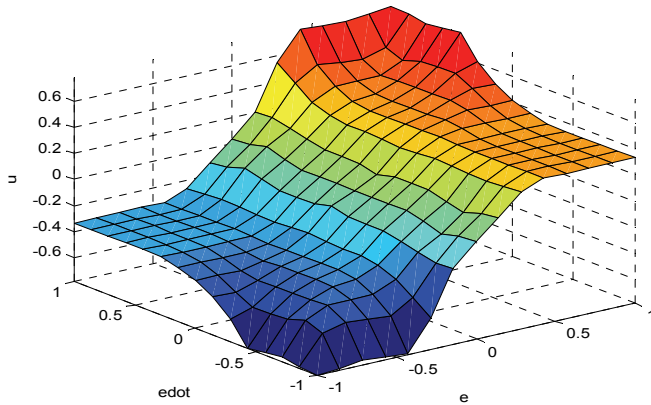


Fig. 5. Control surface of the fuzzy controller.

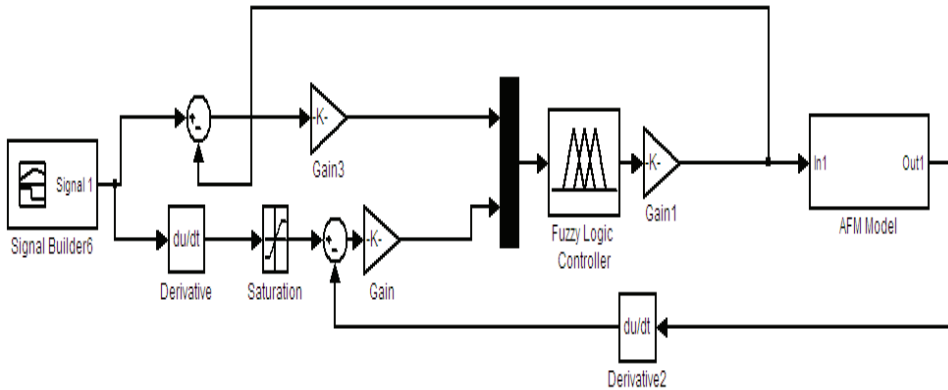


Fig. 6. Simulink block diagram of the system and the fuzzy controller.

$e \setminus \dot{e}$	<b>NB</b>	<b>NS</b>	<b>PS</b>	<b>PB</b>
<b>NB</b>	NB	NB	NS	NS
<b>NS</b>	NB	NS	NS	NS
<b>PS</b>	PS	PS	PS	PB
<b>PB</b>	PS	PS	PB	PB

Table 2. Tabulated Fuzzy Rules.

#### 4. Design of the PD-fuzzy controller

To improve the performance of the PD controller proposed in (Leang & Devasia, 2007) against external disturbances and increase the operation bandwidth of the control system, we used Mamdani fuzzy control to design a PD-fuzzy controller that will automatically tune the gains. Figure 7 shows the block diagram of the controller.

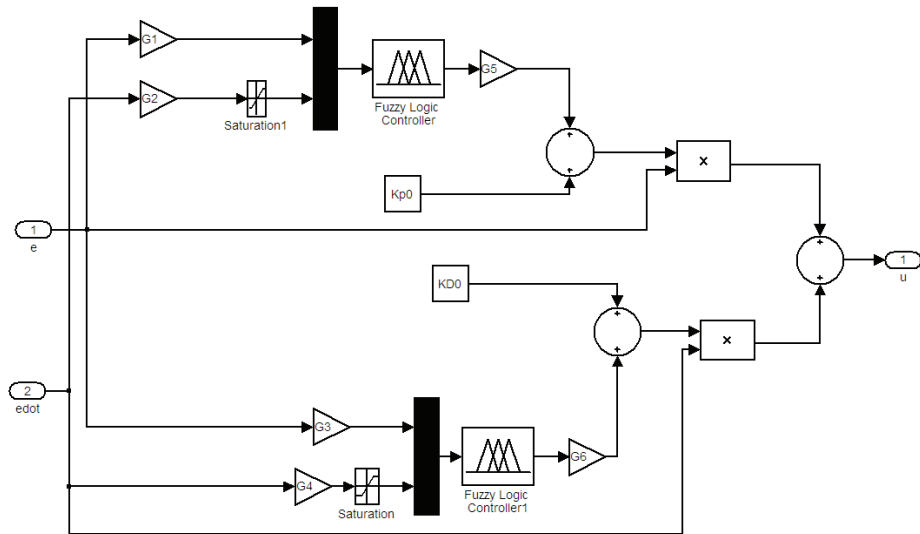


Fig. 7. Block diagram of the PD- fuzzy controller.

In this controller, the standard PD control law:

$$u = u_1 + u_2 \tag{5}$$

where  $u_1$  is the proportional control input and  $u_2$  is the derivative control input, is replaced with:

$$u(t) = (k_{p0} + Fk_p)e(t) + (k_{D0} + Fk_D)\dot{e}(t) \tag{6}$$

where  $k_{p0} = 5000$  and  $k_{D0} = 10$  are fixed gains acting as the nominal values of the PD controller. The value of  $Fk_p$  and  $Fk_D$  are to be determined by fuzzy logic based on the system inputs and added to the nominal gains. Figure 7 shows the manner of adding fuzzy parts of proportional and derivative parts of the PD-Fuzzy control input. After that  $Fk_p$  and  $Fk_D$  are constructed by fuzzy logic section they are added to fixed proportional and derivative gains. The fuzzy logic part of the system is designed to improve the robustness of the PD control system against parameter uncertainties and external disturbances. Table 3 lists the scaling factors which are shown in Figure 7 and used in the PD-Fuzzy control system. Figures 8-10 show the membership functions of the inputs and output of the hybrid PD-Fuzzy controller. Figure 11 shows the control surface of the controller. The error input dominates the output of the fuzzy control indicating that the fuzzy-side of the controller has to compensate particularly for deficiencies in proportional gain.

$G_1=4e7$	$G_2=1250$	$G_3=8e6$
$G_4=250$	$G_5=10000$	$G_6=100$

Table 3. Scaling Factors.

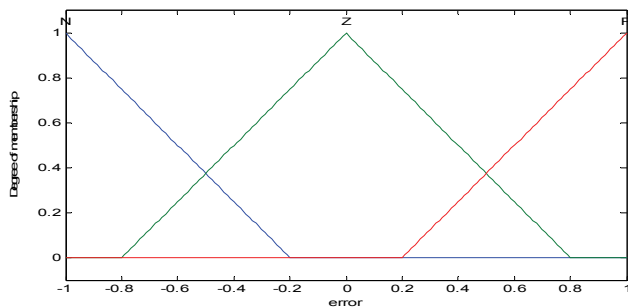


Fig. 8. Error membership functions for the PD-Fuzzy controller.

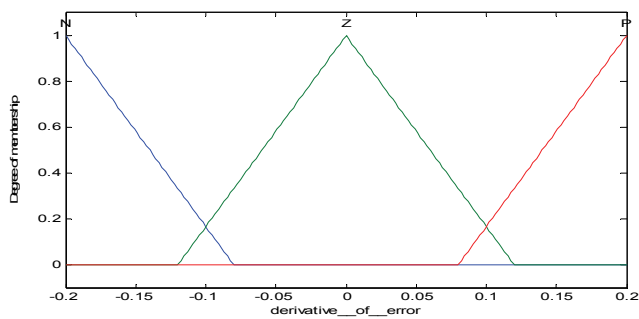


Fig. 9. Error derivative membership functions for the PD-Fuzzy controller.

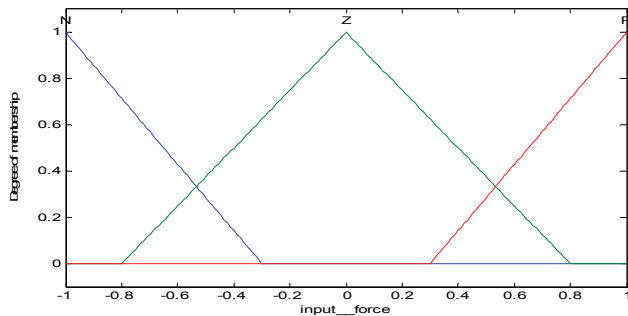


Fig. 10. Output membership functions for the PD-Fuzzy controller.

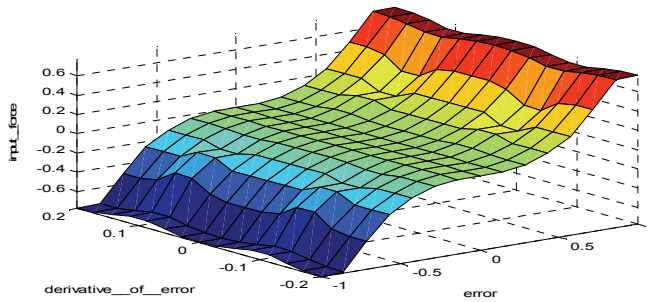


Fig. 11. Control surface of the PD-Fuzzy controller.

## 5. Results

A set of simulated tests was designed to compare the efficiency of the proposed controllers against that of the controller proposed in (Leang & Devasia, 2007). The tests were conducted on an AFM probe [19] with the following specifications: Length=225  $\mu\text{m}$ , Width=45  $\mu\text{m}$ , Thickness=2.5  $\mu\text{m}$ , and tip radius  $R = 5 \text{ nm}$ . Also,  $\rho = 2330 \text{ kg/m}^3$  and  $E^* = 1.69 \times 10^{11} \text{ N/m}^2$ . According to these dimensions and parameters, the lumped stiffness was found by:

$$k = \frac{3E^*I}{L^3} \quad (7)$$

$$m = \rho LA \quad (8)$$

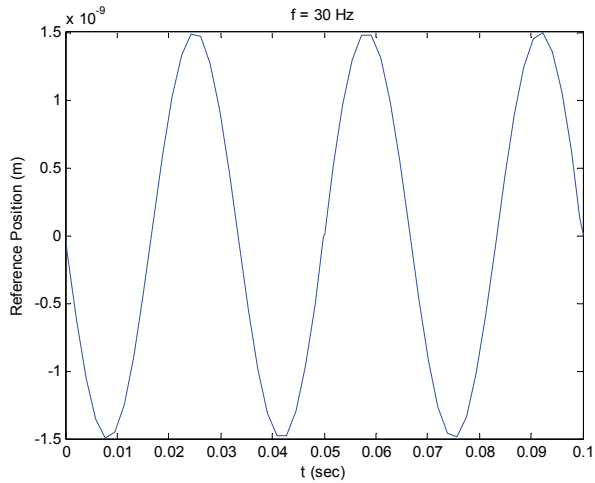
So,  $m=5.89\text{e-}11 \text{ Kg}$  and  $k = 2.6 \text{ N/m}$  and  $f=33.5 \text{ KHz}$ . We conducted three sets of tests imposing progressively more stringent demands on the controllers' performance.

### 5.1 Test one

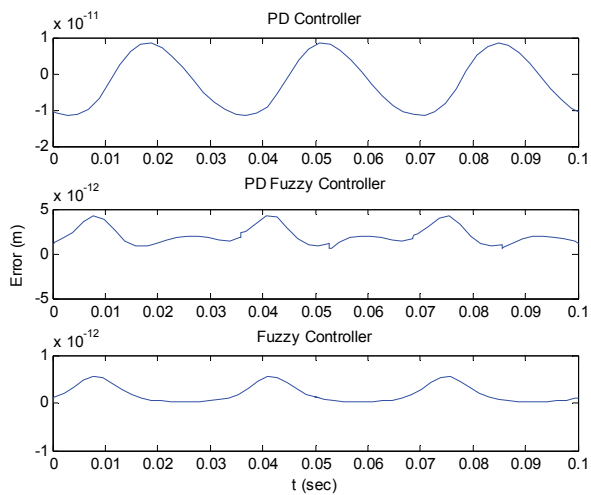
The controller performance was investigated for a sinusoidal terrain and sinusoidal tip displacement trajectory for a range of scan rates from 0.3  $\mu\text{m/s}$  to 15  $\mu\text{m/s}$ . The AFM is traversing in the sinusoidally varying grating with a pitch of 10 nm, resulting in frequencies of encounter varying from 30 Hz to 1500Hz. Figures 12-15 show the tracking-error using the high gain PD controller, the PD-fuzzy, and the fuzzy controllers for 30 Hz, 200 Hz, 500 Hz and 1500Hz, respectively. We found that the tracking-errors of the fuzzy and PD-fuzzy controllers were consistently better than that of the PD controller. In comparison between the fuzzy controller and PD-fuzzy controller, we found that the fuzzy controller had consistently smaller tracking-errors. On the other hand, the fuzzy controller assumes that the plant can supply infinite power, while the PD-fuzzy sets the gains at practically attainable power levels.

However, Figure 13(b) shows that the abrupt gain changes in the PD-fuzzy controller can induce oscillations in the tip position. With this drawback in mind and considering the results obtained in (Salapaka et al., 2005) and (Leang & Devasia, 2007), it is concluded that the PD-fuzzy controller has a very good response that balances error minimization against limiting demands on the plant.



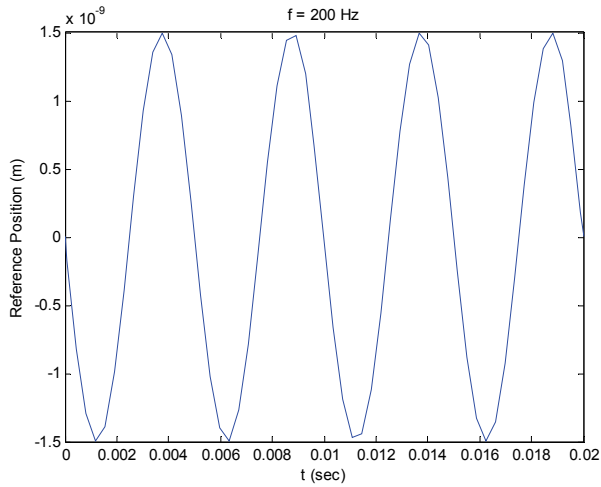


a) Reference signal

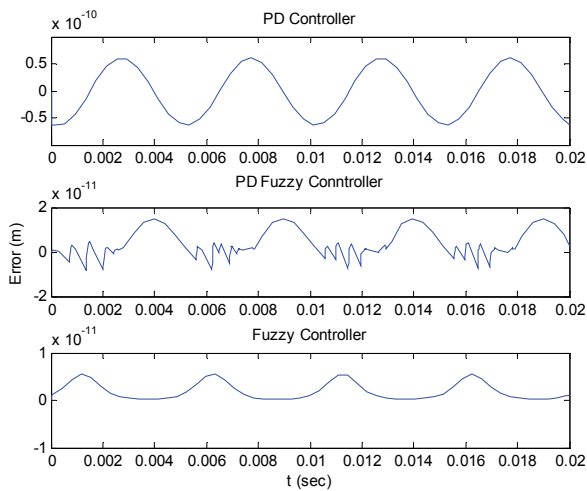


b) Error signals

Fig. 12. Tip tracking-error using PD, PD-Fuzzy, and Fuzzy controllers at an encounter frequency of 30 Hz.

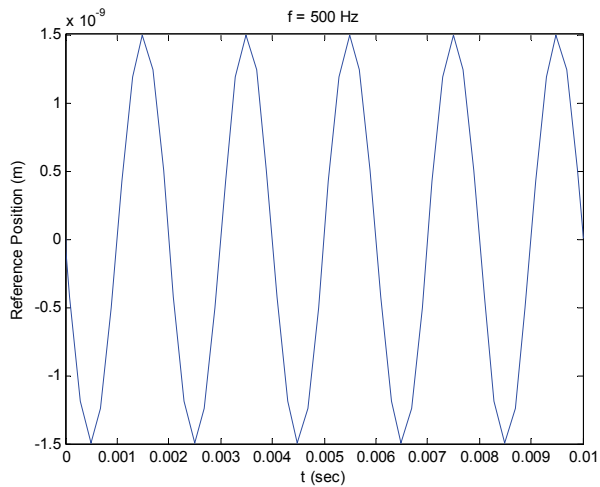


a) Reference signal

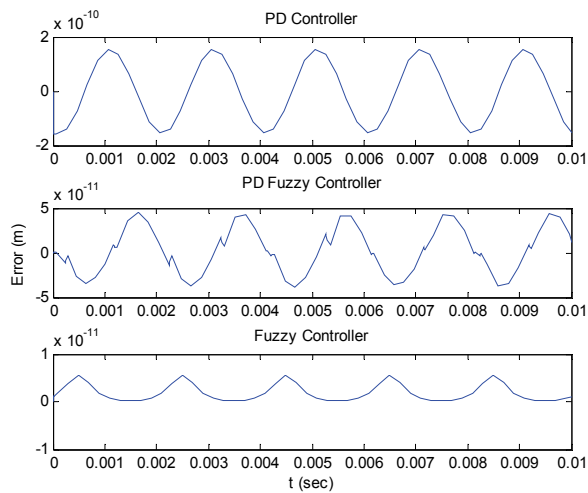


b) Error signals

Fig. 13. Tip tracking-error using PD, PD-Fuzzy, and Fuzzy controllers at an encounter frequency of 200 Hz.

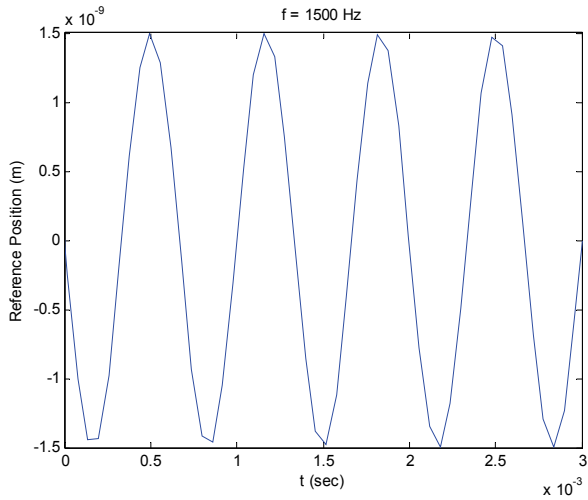


a) Reference signal

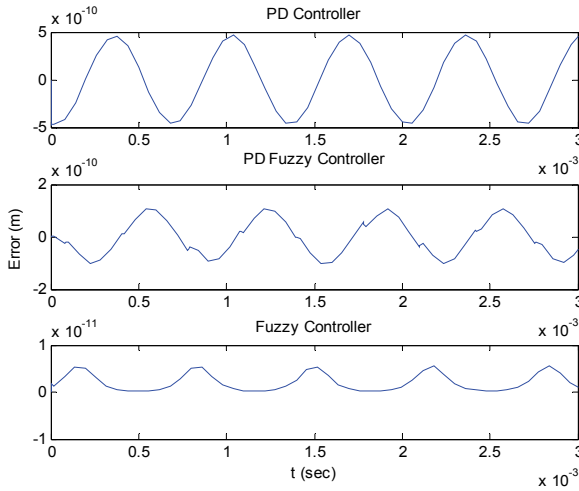


b) Error signals

Fig. 14. Tip tracking-error using PD, PD-Fuzzy, and Fuzzy controllers at an encounter frequency of 500 Hz.



a) Reference signal



b) Error signals

Fig. 15. Tip tracking-error using PD, PD-Fuzzy, and Fuzzy controllers at an encounter frequency of 1500 Hz.

We use the root-mean-square of the error (erms) (Leang & Devasia, 2007):

$$e_{rms}(\%) = \left( \frac{\sqrt{\frac{1}{T} \int_0^T e^2(t) dt}}{\max(x_{ref}) - \min(x_{ref})} \right) \times 100\% \quad (7)$$

As a figure-of-merit to quantify the performance of each of the controllers. Tab.4 lists the tracking root-mean-square error for each controller in each of the test cases above as a percentage of the total output range (3 nm). We find that the performance of the fuzzy and fuzz-PD controllers are consistently, at least, one-order of magnitude, better than that of the PD controller.

Frequency (Hz) \ Controller	PD	PD-Fuzzy	Fuzzy
30	.3	.0638	0.044
200	1.53	.14	0.069
500	3.67	.58	0.084
1500	10.12	1.62	0.1

Table 4. Tracking-error performance for sinusoidal trajectories  $e_{rms}(\%)$ .

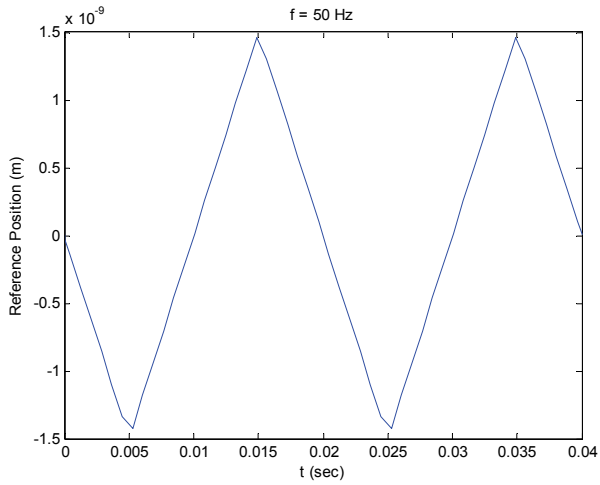
## 5.2 Test two

This simulation examines the tip response to a triangular terrain resulting in the tip displacement trajectories shown in Figures 16(a) and 17(a). The figures show the tracking-error for scan rates of 0.5  $\mu\text{m/s}$  and 2  $\mu\text{m/s}$ , respectively, resulting in encounter frequencies of 50 Hz and 200 Hz. We find that the abrupt position changes in the trajectory result in similar error levels for the PD and the PD-fuzzy controllers that are twice as large as those seen in the fuzzy controller. However, away from these sharp position changes the PD-fuzzy controller performs better than the PD controller. When we compare the results obtained as well as those in (Salapaka *et al.*, 2005) and (Leang & Devasia, 2007), we conclude that both fuzzy and PD-fuzzy controller offer enhanced AFM tip tracking performances.

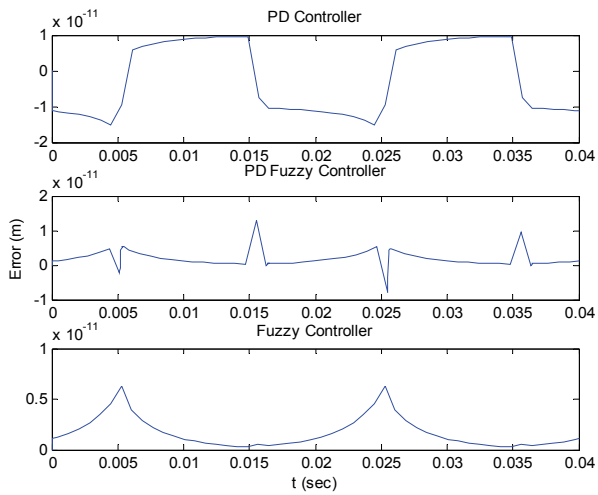
Tab.5 shows the tracking root-mean-square error for each controller in the two test cases. While the PD-fuzzy controller has smaller errors than that of the PD controller, they are of the same order, whereas the error of the fuzzy controller is one order of magnitude smaller than both of them.

Frequency (Hz) \ Controller	PD	PD-Fuzzy	Fuzzy
50	.35	.11	.07
200	1.31	.42	.075

Table 5. Tracking-error performance for triangular trajectories  $e_{rms}(\%)$ .

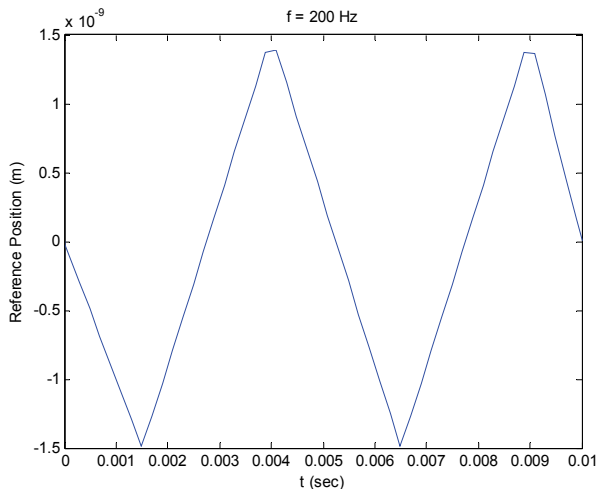


a) Reference signal

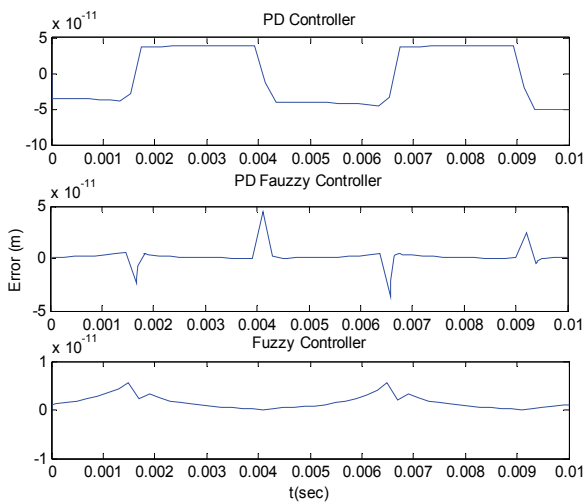


b) Error signals

Fig. 16. AFM response with 50 Hz.



a) Reference signal



b) Error signals

Fig. 17. AFM response with 200 Hz.

### 5.3 Test three

We investigate the response of the controllers to a train of sharp terrain changes resulting in a tip trajectory similar to that shown in Figure 18(a), while the AFM is scanning at a rate of  $1 \mu\text{m/s}$ . This condition represents a more general specimen surface with irregular and sharp height changes representing the asperities of the surface. The error in the fuzzy controller is one-order of magnitude smaller than those of the PD and PD-fuzzy controllers. The PD-Fuzzy controller tracking-error is smaller both in absolute and average senses than that of the PD controller as shown in Figure 18(b) and Tab.6, respectively.

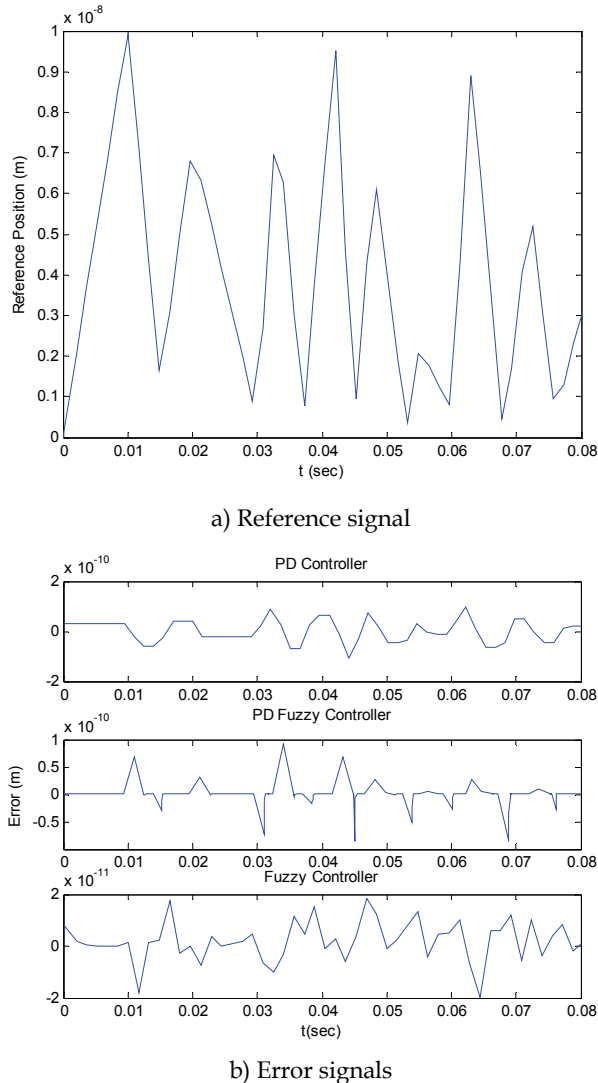


Fig. 18. AFM response in random reference.



PD	PD-Fuzzy	Fuzzy
.46	.15	.08

Table 6. Tracking-error performance for the random trajectory  $e_{rms}(\%)$ .

## 6. Conclusion

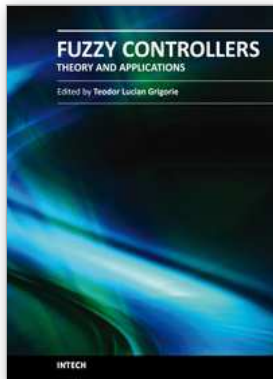
In this paper we used fuzzy control theory to design two controllers for closed-loop feedback control of an AFM probe. These controllers are designed based on conventional fuzzy Mamdani control theory and the introduction of a fuzzy controller to a PD controller to tune online the PD gains resulting in a hybrid PD-fuzzy controller. Comparing the results of these controllers and a baseline a high-gain PD controller, we found that the fuzzy controller had the best position-tracking performance. However since it imposes unrealistic power demands on the AFM plant, it was concluded that the PD-fuzzy controller represents the best balance between minimization of the tracking-error and realistic power demands on the plant.

Since the PD-fuzzy controller had smaller tracking-error than other controllers reviewed in this chapter, it allows the AFM to operate at faster scanning rates, resulting in wider bandwidth of encounter frequencies, for the same error tolerance levels. Finally, it was found that the PD-fuzzy controller can induce oscillations in the position of the probe tip. Therefore, we recommend enhancing the PD-fuzzy controller to mitigate this negative effect of abrupt changes in the PD controller gains.

## 7. References

- Ashhab, M.; Salapaka, M.V.; Dahleh, M. & Mezić, I. (1999). Melnikov-Based Dynamical Analysis of Microcantilevers in Scanning Probe Microscopy, *Nonlinear Dynamics*, Vol. 20, PP. 197-220.
- Barrett, R. C. & Quate, C. F. (1991). Optical scan-correction system applied to atomic force microscopy, *Rev. Sci. Instrum.*, Vol. 62, PP. 1393-1399.
- Binnig, G.; Gerber, C. & Quate, C. (1986). Atomic force microscope, *Phys. Rev. Lett.*, Vol. 56, PP. 930-933.
- Devasia, S.; Eleftheriou, E. & Moheimani, S. O. R. (2007). A Survey of Control Issues in Nanopositioning, *IEEE Trans. Ctrl. Sys. Tech.*, Vol. 15, PP. 802-823.
- Fang, Y.; Feemster, M.; Dawson, D. & Jalili, N.M. (2005). Nonlinear control techniques for an atomic force microscope system, *Control Theory & Applications Journal*, Vol. 3, PP. 85-92.
- Jalili, N.; Dadfarnia, M. & Dawson, D. M. (2004). A Fresh Insight Into the Microcantilever Sample Interaction Problem in Non-Contact Atomic Force Microscopy, *Journal of Dynamic Systems, Measurement, and Control*, Vol. 126, PP. 327-335.
- Jung, H. & Gweon, D. G. (2000). Creep characteristics of piezoelectric actuators, *Rev. Sci. Instrum.*, Vol. 71, PP. 1896-1900.
- Leang, K. K. & Devasia, S. (2007). Feedback-Linearized Inverse Feedforward for Creep, Hysteresis, and Vibration Compensation in AFM Piezoactuators, *IEEE Trans. Ctrl. Sys. Tech.*, Vol. 15, PP. 927-935.

- Pao, L. Y.; Butterworth, J. A. & Abramovitch, D. Y. (2007). Combined Feedforward/Feedback Control of Atomic Force Microscopes, *Proceedings of the 2007 American Control Conference*, USA, July 2007, New York.
- Rifai, O. M. El. & Toumi, K. Y. (2004). On Automating Atomic Force Microscopes: An Adaptive Control Approach, *43rd IEEE Conference on Decision and Control*, December 2004 Atlantis, Paradise Island, Bahamas.
- Salapaka, S. M.; De, T. & Sebastian, A. (2005). A Robust Control Based Solution to the Sample-Profile Estimation Problem in Fast Atomic Force Microscopy, *Int. J. Robust Nonlinear Control*, Vol. 15, PP. 821-837.
- Salapaka, S.M.; Sebastian, A.; Cleveland, J. P. & Salapaka, M. V. (2002). High Bandwidth Nano-Positioner: A Robust Control Approach, *Rev. Sci. Instr.*, 2002.
- Schitter, G.; Stark, R. W. & Stemmer, A. (2004). Fast Contact-Mode Atomic Force Microscopy on Biological Specimen by Model-Based Control, *Ultramicroscopy*, Vol. 100, PP. 253-257.
- Schitter, G.; Stark, R. W. & Stemmer, A. (2004). Identification and Open- Loop Tracking Control of a Piezoelectric Tube Scanner for High- Speed Scanning-Probe Microscopy, *IEEE Trans. Ctrl. Sys. Tech.*
- Schitter, G.; Menold, P. H.; Knapp, H. F.; Allgöwer, F. & Stemmer, A. (2001). High Performance Feedback for Fast Scanning Atomic Force Microscopes, *Rev. Sci. Instr.*, Vol. 72.
- Sebastian, A.; Gannepalli, A. & Salapaka, M. V. (2007). A Review of the Systems Approach to the Analysis of Dynamic-Mode Atomic Force Microscopy, *IEEE Trans. Ctrl. Sys. Tech.*, Vol. 15, PP. 952-959.
- Sebastian, A.; Salapaka, M.V. & Cleveland, J. P. (2003). Robust Control Approach to Atomic Force Microscopy, *Proceedings of the 42nd IEEE Conference on Decision and Control*, USA, December 2003, Maui, Hawaii.
- Sinha, A. (2005). Nonlinear dynamics of atomic force microscope with PI feedback, *Journal of Sound and Vibration*, Vol. 288, PP. 387-394.



## **Fuzzy Controllers, Theory and Applications**

Edited by Dr. Lucian Grigorie

ISBN 978-953-307-543-3

Hard cover, 368 pages

**Publisher** InTech

**Published online** 28, February, 2011

**Published in print edition** February, 2011

Trying to meet the requirements in the field, present book treats different fuzzy control architectures both in terms of the theoretical design and in terms of comparative validation studies in various applications, numerically simulated or experimentally developed. Through the subject matter and through the inter and multidisciplinary content, this book is addressed mainly to the researchers, doctoral students and students interested in developing new applications of intelligent control, but also to the people who want to become familiar with the control concepts based on fuzzy techniques. Bibliographic resources used to perform the work includes books and articles of present interest in the field, published in prestigious journals and publishing houses, and websites dedicated to various applications of fuzzy control. Its structure and the presented studies include the book in the category of those who make a direct connection between theoretical developments and practical applications, thereby constituting a real support for the specialists in artificial intelligence, modelling and control fields.

### **How to reference**

In order to correctly reference this scholarly work, feel free to copy and paste the following:

Amir Farrokh Payam, Eihab M. Abdel Rahman and Morteza Fathipour (2011). Control of Atomic Force Microscope Based on the Fuzzy Theory, Fuzzy Controllers, Theory and Applications, Dr. Lucian Grigorie (Ed.), ISBN: 978-953-307-543-3, InTech, Available from: <http://www.intechopen.com/books/fuzzy-controllers-theory-and-applications/control-of-atomic-force-microscope-based-on-the-fuzzy-theory>

# **INTECH**

open science | open minds

### **InTech Europe**

University Campus STeP Ri  
Slavka Krautzeka 83/A  
51000 Rijeka, Croatia  
Phone: +385 (51) 770 447  
Fax: +385 (51) 686 166  
[www.intechopen.com](http://www.intechopen.com)

### **InTech China**

Unit 405, Office Block, Hotel Equatorial Shanghai  
No.65, Yan An Road (West), Shanghai, 200040, China  
中国上海市延安西路65号上海国际贵都大饭店办公楼405单元  
Phone: +86-21-62489820  
Fax: +86-21-62489821

© 2011 The Author(s). Licensee IntechOpen. This chapter is distributed under the terms of the [Creative Commons Attribution-NonCommercial-ShareAlike-3.0 License](#), which permits use, distribution and reproduction for non-commercial purposes, provided the original is properly cited and derivative works building on this content are distributed under the same license.